



**HAL**  
open science

## **Analysis of the LIF/Mie droplet sizing technique applied to an aeronautical engines spray**

Sébastien Garcia, Christine Lempereur, Pierre Doublet, Mikael Orain, Jérôme Anthoine

### ► **To cite this version:**

Sébastien Garcia, Christine Lempereur, Pierre Doublet, Mikael Orain, Jérôme Anthoine. Analysis of the LIF/Mie droplet sizing technique applied to an aeronautical engines spray. ILASS Europe 2022, Sep 2022, Online, Israel. <hal-03910035>

**HAL Id: hal-03910035**

**<https://hal.science/hal-03910035v1>**

Submitted on 21 Dec 2022

**HAL** is a multi-disciplinary open access archive for the deposit and dissemination of scientific research documents, whether they are published or not. The documents may come from teaching and research institutions in France or abroad, or from public or private research centers.

L'archive ouverte pluridisciplinaire **HAL**, est destinée au dépôt et à la diffusion de documents scientifiques de niveau recherche, publiés ou non, émanant des établissements d'enseignement et de recherche français ou étrangers, des laboratoires publics ou privés.



HAL Authorization

# Analysis of the LIF/Mie Droplet Sizing Technique Applied to an Aeronautical Engines Spray.

S. Garcia\*<sup>1</sup>, C. Lempereur<sup>1</sup>, P. Doublet<sup>1</sup>, M. Orain<sup>1</sup> and J. Anthoine<sup>1</sup>

<sup>1</sup>ONERA / DMPE, Toulouse University, F-31055 Toulouse - France

\*Corresponding author: [sebastien.garcia@onera.fr](mailto:sebastien.garcia@onera.fr)

## Abstract

The LIF/Mie droplet sizing technique has been studied for many years, but its implementation remains challenging due to the fact that the usual assumptions behind it are not valid in practice. Not only the scattered light intensity is not proportional to the droplet surface area, but also single light scattering is not preserved in dense sprays. To overcome these limitations, an innovative experimental setup has been developed, including a 1p-SLIPI device. An ethanol spray (seeded with rhodamine 6G) generated from a Delavan nozzle is investigated under ambient conditions.

## Keywords

Aeronautical Sprays, Optical Diagnostic, LIF/Mie Technique, Multiple Scattering, 1p-SLIPI.

## Introduction

The Sauter Mean Diameter, also called the surface-volume diameter, is frequently used to characterize injection devices in aeronautical gas turbines. It estimates the mean size of a given particle distribution and is defined as the diameter of a sphere that has the same volume/surface area ratio as the particles of interest [1]. The SMD is a key factor for mass transfer processes: a small SMD indicates fine evaporation, weak penetration and efficient mixture. The application of CFD codes to such unsteady and dense sprays is still challenging; if numerical parameters need to be tuned to fit experimental results, these data must in turn be reliable. In this respect, experiments yield essential information for the development and evaluation of atomization and spray flow models.

In order to fulfill the accuracy requirement, laser-based optical diagnoses are in steady progress. Although a classical pointwise technique, Phase Doppler Anemometry (PDA), has been widely investigated over the last decades, whole-field measurement techniques are a promising mean to reduce the test duration and cost. In this context, the Planar Droplet Sizing (PDS) method, also called LIF/Mie ratio, is a planar laser imaging method developed by Yeh & al. [2] and used to obtain spray granulometry. This technique is based on Mie scattering and fluorescence emission from droplets. The Mie scattering is essentially based on elastic light scattering phenomenon by spherical particles. In that theory, for the droplets whose diameter is larger than the emission wavelength, scattered intensity is proportional to the particles square diameter (i.e.  $I_s \propto D^2$ ). Contrary to Mie scattering, the laser induced fluorescence (LIF) method is based on inelastic light emission. Liquid fluorescence is only achieved if the liquid contains fluorescent molecules. If not, it must be seeded with a fluorescent dye. According to Felton & al [3], the LIF signal is proportional to the fluorescent molecule concentration which depends on liquid volume. Thereby, fluorescence emission from the droplets is proportional to their cubic diameter (i.e.  $I_f \propto D^3$ ). The SMD is then obtained by applying the ratio of the two intensities (fluorescence and scattering) :

$$\frac{I_f}{I_s} = \frac{k_f \sum_i^N D_i^3}{k_s \sum_i^N D_i^2} = K.SMD \quad (1)$$

An important limitation of the PDS technique is the application to a dense spray. Indeed, in a low-density spray, the application of laser imaging is possible because the single scattering hypothesis predominates. However, in the case of a dense spray (Optical Depth [OD] > ±5), the light undergoes several scattering events before reaching the camera sensor. Thereby, the Lorenz-Mie theory is no longer relevant because the scattered intensity is no longer proportional to the droplet diameter. To

overcome that multiple scattering issue and for instantaneous imaging of a transient spray, a new method named Structured Laser Illumination Planar Imaging (SLIPI) has been developed [4,5]. This technique is based on laser sheet imaging and structured illumination.

### Focus of the study

The aim of this paper is to study the parameters that can alter the reliability of the droplet sizing technique applied to an aeronautical spray. The actual implementation of the technique is presented first. Subsequently, a light extinction calculation in the spray is performed to estimate the spray density through the OD parameter. In the following section, given that both LIF and Mie signals have been demonstrated to not be proportional respectively to the droplet volume and surface area, a more theoretical analysis of fluorescence emission and light scattering is undertaken. The use of a TwinCam device and a telecentric objective for the application of the PDS method proves to be essential. Finally, a calibration method based on a look-up table is proposed in order to obtain SMD mapping of the spray.

### Experimental setup

The injection setup is an industrial one used in the combustion chamber of a helicopter engine. The droplet generator (Delavan, SIMPLEX 60°, type hollow cone) produces monodisperse droplets of sizes ranging between approximately 10  $\mu\text{m}$  to 100  $\mu\text{m}$ . Experiments are conducted at ambient temperature and atmospheric pressure on the unsteady spray generated downstream of the injector. The liquid used for the experiment is ethanol and the mass flow rate is set to 2,20 g/s.

The optical setup for PDS measurement is shown in **Figure 1**. A laser beam generated by a frequency-doubled Nd: YAG - 532nm pulsed Laser (Quantel Twins Big Sky 200mJ, 10Hz, 8ns impulsion) was converted into a light sheet by the 1p-SLIPI module [5]. The laser is placed above the experiment and a mirror is used to redirect the laser sheet through the spray.

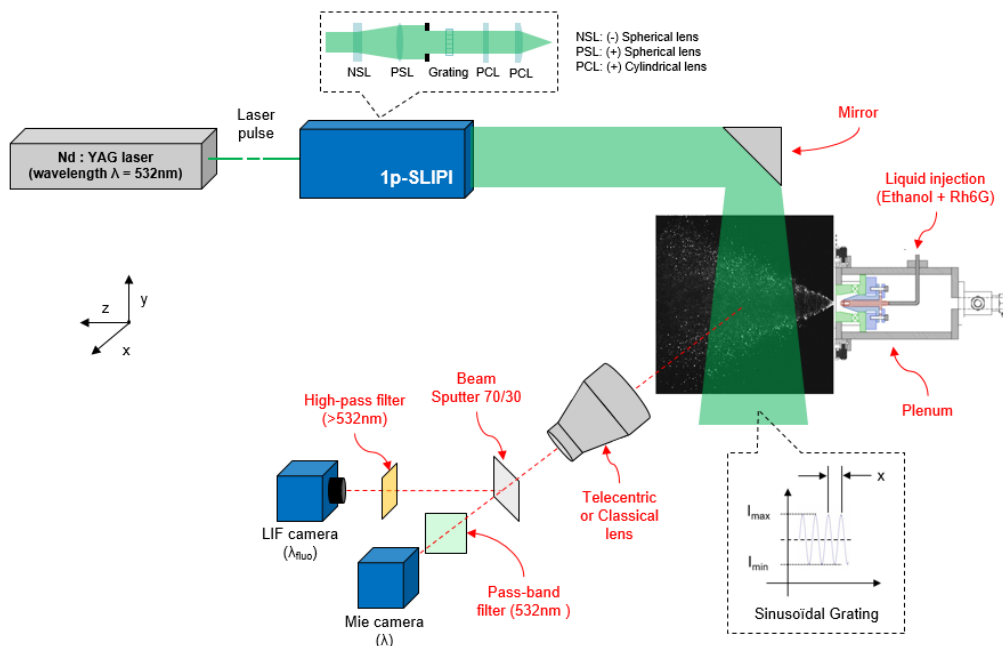


**Figure 1.** View of the optical LIF/Mie droplet sizing arrangement (PDS).

To collect the LIF and Mie signals from the spray, the reception module views the experiment at an angle of 90°. A classical objective (Nikon Micro-Nikkor - 60 mm - f/2.8) is first used and highlights the angular dependence of scattered light intensity within the field of view. A comparison is done with a telecentric objective (OPTO Engineering\_TC1MHR080-C) to overcome this angular variation. Two sCMOS cameras (PCO edge 4.2) are coupled to the single objective by a TwinCam device (CAIRN Research). This optical arrangement enables a perfect superimposition of both

images and suppresses any discrepancy that may come from different optical paths. This experimental configuration allows simultaneous LIF and Mie measurements.

As previously discussed, the PDS technique requires a fluorescent liquid. Since ethanol is not fluorescent when excited at 532nm, a soluble dye has to be added. Rhodamine 6G (Rh6G) is selected because it is the most efficient under these experimental conditions. Since the emission spectrum of Rh6G lies beyond the excitation wavelength up to 650 nm, the LIF camera needs a specific long pass edge filter (Semrock BLP532), offering an exceptional laser line blocking ( $OD > 7$  at 532 nm) and high transmission ( $> 95\%$  above 541 nm). This ensures that there is no contamination from scattered light in the image acquired by this camera. The MIE camera is equipped with a 532 nm band pass filter (FWHM 10 nm). A beam splitter (Chroma, non-polarizing 70/30) is used to redirect the light to the cameras. Since the fluorescence signal intensity is less important than the scattering one, the beam splitter returns 70% of the signal to the LIF camera and 30% to the Mie camera. The two filters and the beam splitter are located inside the TwinCam.

### Extinction of light through the spray

The extinction of light through the spray of droplets along the laser path, from top to bottom of the image, results from absorption and scattering. Considering  $I(0)$  the initial intensity of the incident light, its value  $I(x)$  after having crossed a distance  $x$  through the medium is derived from the OD. This parameter can be estimated from the local particle concentration and size:

$$I(x) = I(0) e^{-OD} = I(0) e^{-N \cdot \sigma_e \cdot x} \quad (2)$$

$$OD = N \cdot \sigma_e \cdot x \approx N \cdot Q_e \cdot \sigma_g \cdot x \approx N \cdot Q_e \cdot \frac{\pi \cdot D^2}{4} \cdot x \quad (3)$$

Where  $N$  is the number of particles per unit volume [ $\#/m^3$ ],  $\sigma_e$  is the extinction cross section [ $m^2$ ],  $Q_e$  is the extinction efficiency factor,  $\sigma_g$  is the geometrical cross section [ $m^2$ ] and  $D$  is the diameter of the particles [ $m$ ]. The extinction efficiency factor calculated for  $n = 1.36 + i \cdot 10^{-6}$  (ethanol) and  $\lambda = 532$  nm is close to 2 in the diameter range of interest. A numerical application integrating concentration and size data from the PDA measurement along vertical Y-profiles is undertaken to estimate the attenuation of the laser intensity through the spray (**Figure 2**).

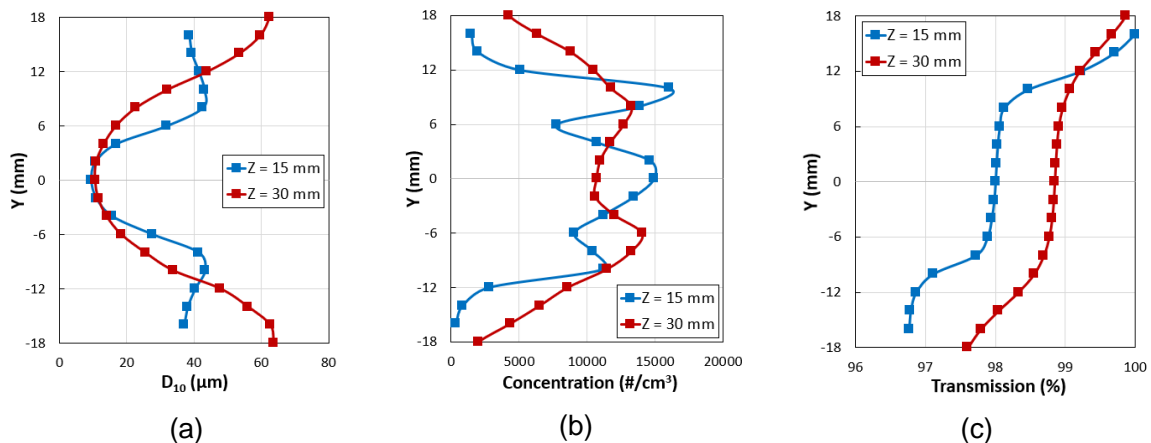


**Figure 2.** (a) Droplet mean diameter, (b) concentration and (c) transmission of light intensity through the spray at  $Z = 15$  mm &  $Z = 30$  mm from the injector.

**Figure 2 (c)** shows a global decrease in transmission when the light beam crosses the spray. This low signal attenuation is explained by the low OD estimated over the entire spray ( $OD < 1$ ). Globally, the medium is not optically dense under the experimental conditions of interest.

### Influence of the dye concentration on LIF imaging

The fluorescence emission is assumed to be isotropic: intensity does not depend on the viewing angle around the droplet. According to Felton & al [3], the main parameter that affects the relation

between fluorescence intensity and particle volume is the dye concentration  $C$  [mol/m<sup>3</sup>]. On the one hand, since fluorescent intensity is generally low, it could be tempting to increase the dye concentration. On the other hand, it would correlatively increase the absorption of light through the droplet and make the fluorescent intensity no longer proportional to the droplet volume but to the diameter at a power  $F(C)$  smaller than 3 (Eq.4). The phenomenon becomes all the more sensitive as the diameter increases. That's why, a compromise has to be made on the dye concentration, in order to obtain sufficient fluorescent signal while maintaining a volumetric emission.

$$I_f = I_i k_f \sum n_i D_i^{F(C)} \quad (4)$$

The quantitative influence of dye concentration was studied by Charalampous and Hardalupas [6], who compared numerical and experimental results: they demonstrated that for a Rhodamine 6G concentration up to 10 mg/L, the  $F(C)$  exponent decreases from 3 to 2.95. In our experiments, a concentration of 4 mg/L was sufficient to give an exploitable fluorescent signal on the LIF camera (**Figure 3 (a)**). For this concentration, the value of  $F$  has been estimated via the GMLT (Generalized Lorenz-Mie Theory) software [8]. This software allows to compute in the 3 dimensions of space the excitation field within an illuminated droplet. In this formalism, the drop is considered as a spherical and homogeneous particle. The calculation of the excitation field is performed in the framework of the Generalized Lorenz-Mie Theory. The input data for this code are the refractive index, the extinction coefficient, the diameter of the droplet, the laser excitation wavelength, the width of the laser beam, the position of the drop in the laser beam and the laser polarization. Once the laser excitation field is calculated within the drop, it is spatially integrated over the entire volume of the drop. This step is then repeated for different particle diameters. The analysis of the evolution of the fluorescence intensity as a function of the drop diameter finally allows to estimate the value of the  $F$  coefficient close to 3 (2.98 on **Figure 3 (b)**).

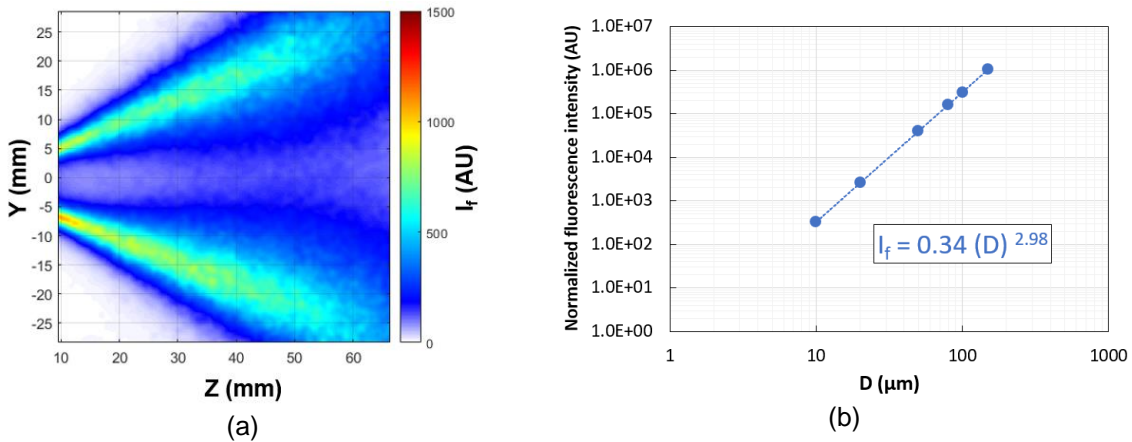


**Figure 3.** (a) Average LIF image, (b) Evolution of fluorescence intensity as a function of particle size.

### Influence of the scattering angle and particle diameter on Mie imaging

The fundamental hypothesis given by Yeh & al. [2], on the proportionality between scattered intensity and the particles square diameter, has been demonstrated by Charalampous & Hardalupas [4] as not valid in practice. Indeed, the scattered intensity  $I_s$  depends on the intensity of the light incident on the particle  $I_i$ , on the particle diameter  $D$ , on its refractive index  $n$  and, most importantly, on the scattering angle  $\alpha$ . As a result, the proportionality relationship becomes:

$$I_s = I_i k_s \sum n_i D_i^{M(D,\alpha,n)} \quad (5)$$

A mean scattering image of the longitudinal section of spray, averaged over 700 images, is presented in **Figure 4 (a)**. The image is not symmetric about the  $Z$  axis. An attenuation of approximately 9 % between the amplitudes of the two peaks A and B can be measured on a

vertical Y-profile at  $Z = 15$  mm from the injector (**Figure 4 (b)**):  $I_{s(B)} = 91\% I_{s(A)}$ . In order to interpret this result, the main parameters that influence the scattered light intensity  $I_s$  will be investigated (Eq. 5). Since the refractive index is constant, the diameter profiles measured by PDA are symmetric about Z (**Figure 2 (a)**) and the extinction of light through the spray (from A to B) is less than 2% and confirmed by the symmetry of the LIF profiles, the only factor that may explain the dissymmetry of  $I_s$  is a variation of  $\alpha$  within the field of view.

This angular dependence can be quantified by means of simulation: the optical axis is at a scattering angle  $\alpha_0 = 90^\circ$  and the total angle of view between A and B is  $\pm 3^\circ$ . The intensity of light scattered by the droplets at locations A ( $\alpha_A = 88,5^\circ$ ) and B ( $\alpha_B = 91,5^\circ$ ) is calculated from the Mie theory in **Figure 7 (a)**, considering the size distribution, the laser wavelength ( $\lambda = 532$  nm) and the refractive index of ethanol ( $n = 1.36 + 4.06e^{-06}$ ). The difference in scattered intensity between A and B is roughly equal to 9 %, which is of the same order of magnitude as the relative intensity drop on the Mie scattering image.

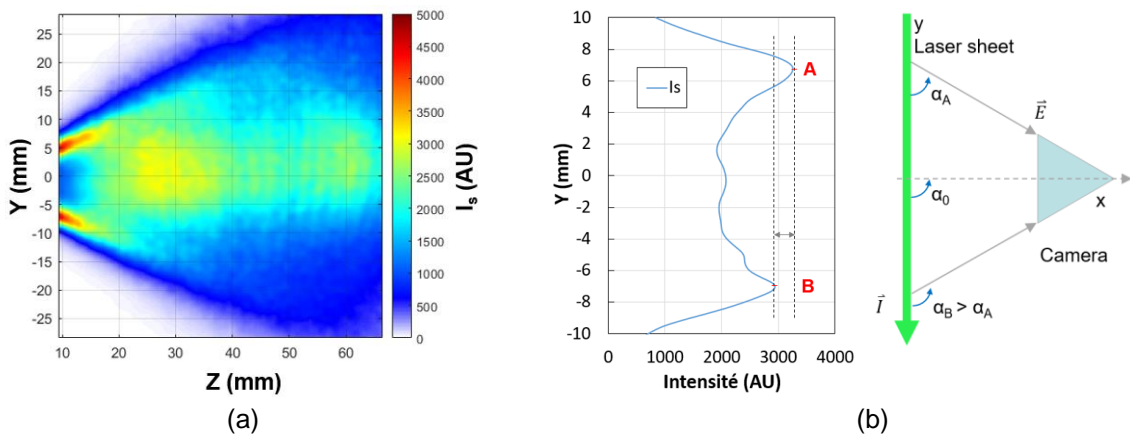


**Figure 4.** Conventional objective : (a) Average Mie scattered light image. (b) Vertical Y-profiles on Mie images at  $Z = 15$  mm from the injection point and definition of the local scattering angle.

This strong angular dependence cannot be corrected by the PDS ratio because it only affects the Mie images and therefore results in a bias on the rPDS values. The experimental results in **Figure 5 (a)** show an average LIF/Mie ratio mapping obtained with a conventional lens. In **Figure 5 (b)**, a dissymmetry of approximately 9 % appears on the rPDS profile at  $Z = 15$  mm.

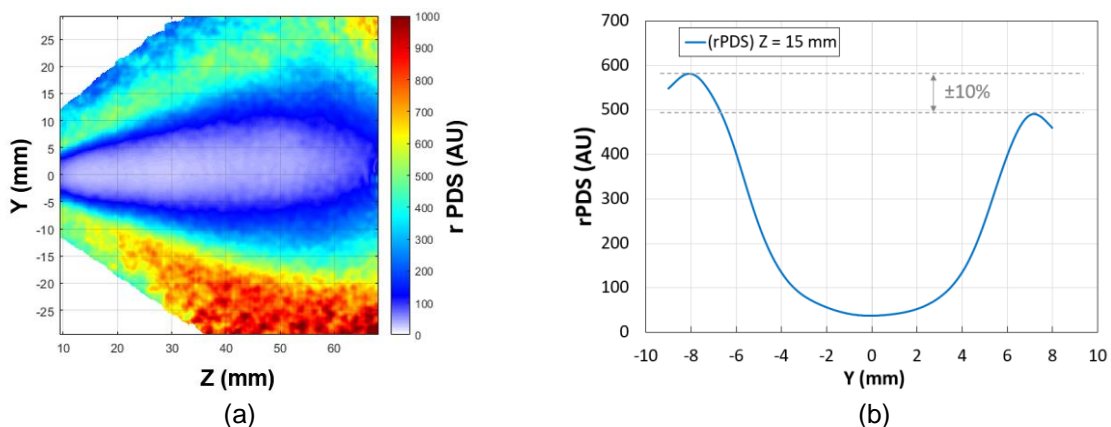


**Figure 5.** (a) Average LIF/Mie ratio maps obtained with 1p-SLIPI and conventional lens. (b) Dissymmetry observed in the rPDS spray at  $Z = 15$  mm.

In order to correct such a phenomenon, an approach consists in generating an image with homogeneously distributed particles and to use it as a flatfield image [7]. But the solution is only applicable if a monodisperse seeding is available. An alternative could be to determine a favorable scattering angle, allowing to reduce the intensity variation in the field of view. Finally, the solution

adopted to remove this angular dependence, is the use of a telecentric objective which only collects parallel or collimated rays that originate from the laser sheet. No angular variation is expected within the field of view. As a result, the intensity profiles on the Mie images are almost symmetrical around the injection axis, as shown in **Figure 6 (b)**. The slight remaining dissymmetry may originate from other physical sources and, most importantly does not result in a dissymmetry of the SMD profiles. In this application, the lens diameter was chosen equal to the size of the field of view (80 mm) and the working distance is fixed to 227 mm.

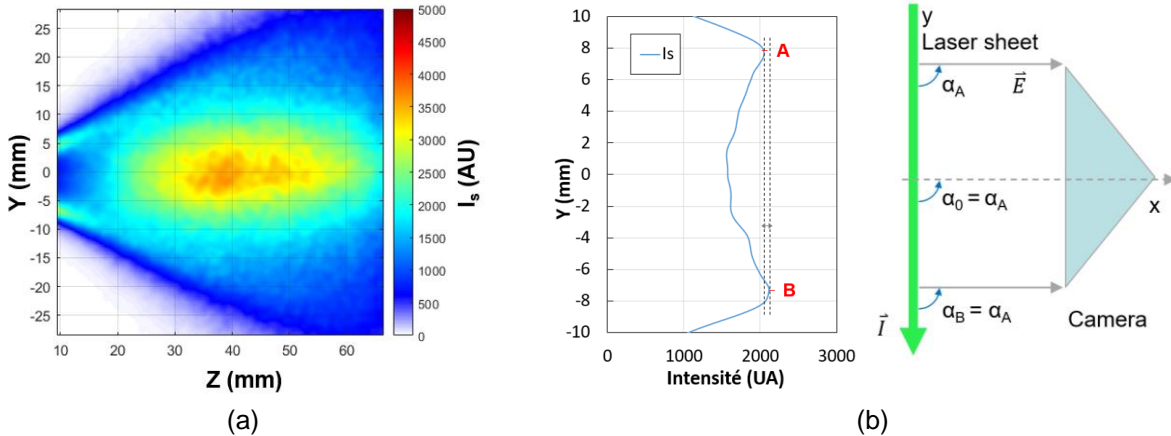


**Figure 6.** Telecentric objective: (a) Mean Mie scattered light image, (b) vertical Y-profiles on Mie images at  $Z = 15$  mm from the injection point and definition of the local scattering angle.

Another parameter that affects the relationship linking the scattered intensity to the drop surface is the droplet diameter  $D$ . In the range of interest (10-100  $\mu\text{m}$ ), the  $D^2$  law is invalidated and the  $S$  exponent steadily increases from 1 to 2 with the diameter. As shown in **Figure 7 (b)**, the best approximation of the  $M$  exponent is 1,7.

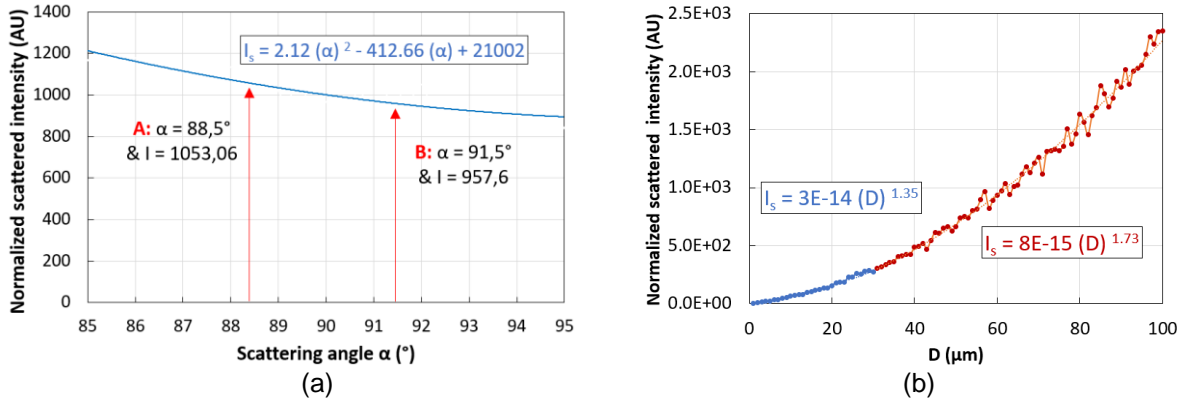


**Figure 7.** (a) Evolution of the scattered intensity as a function of the scattering angle (particle size distribution: 20-80 $\mu\text{m}$ ). (b) Evolution of the scattered intensity as a function of the droplet diameter.

### Calibration of 1p-SLIPI\_PDS method and absolute SMD mapping

The determination of the  $F$  and  $M$  coefficients shows that the  $rPDS$  ratio is not proportional to a diameter:

$$SMD^{PDA} = \frac{\sum_i^N D^3}{\sum_i^N D^2} \rightarrow \text{has the unit of a diameter} \quad (6)$$

$$rPDS = \frac{\sum_i^N D^F}{\sum_i^N D^M} = \frac{\sum_i^N D^{2,98}}{\sum_i^N D^{1,73}} \rightarrow \text{has the unit of a diameter at a power of 1,25} \quad (7)$$

However, for a given spray, the value of the  $M$  coefficient is not valid on the entire diameter range: for diameters below 30  $\mu\text{m}$ , the value of the  $M$  is close to 1,35 (**Figure 7**).

To convert the PDS ratio has the unit of a diameter, the most straightforward method of calibration consists in creating a correspondence between values of SMD ( $\mu\text{m}$ ) measured with PDA and rPDS ratios (AU) obtained by PDS image processing at the same points. A cloud of experimental points can be plotted with rPDS on the abscissa and SMD on the ordinate (**Figure 8 (a) & (b)**). Since the rPDS is not homogeneous to a single diameter, a non-linearity between the two quantities clearly appears: a power law fit can be used to build a Look Up Table (LUT) to transform rPDS images into SMD maps. Initially, a great number of profiles taken at different distances from the injection point were included in the calibration procedure, in order to assess its validity over the largest diameter range. Once the method has been checked, the interest is to limit the time-consuming PDA acquisitions to a few relevant profiles, in order to build the LUT.

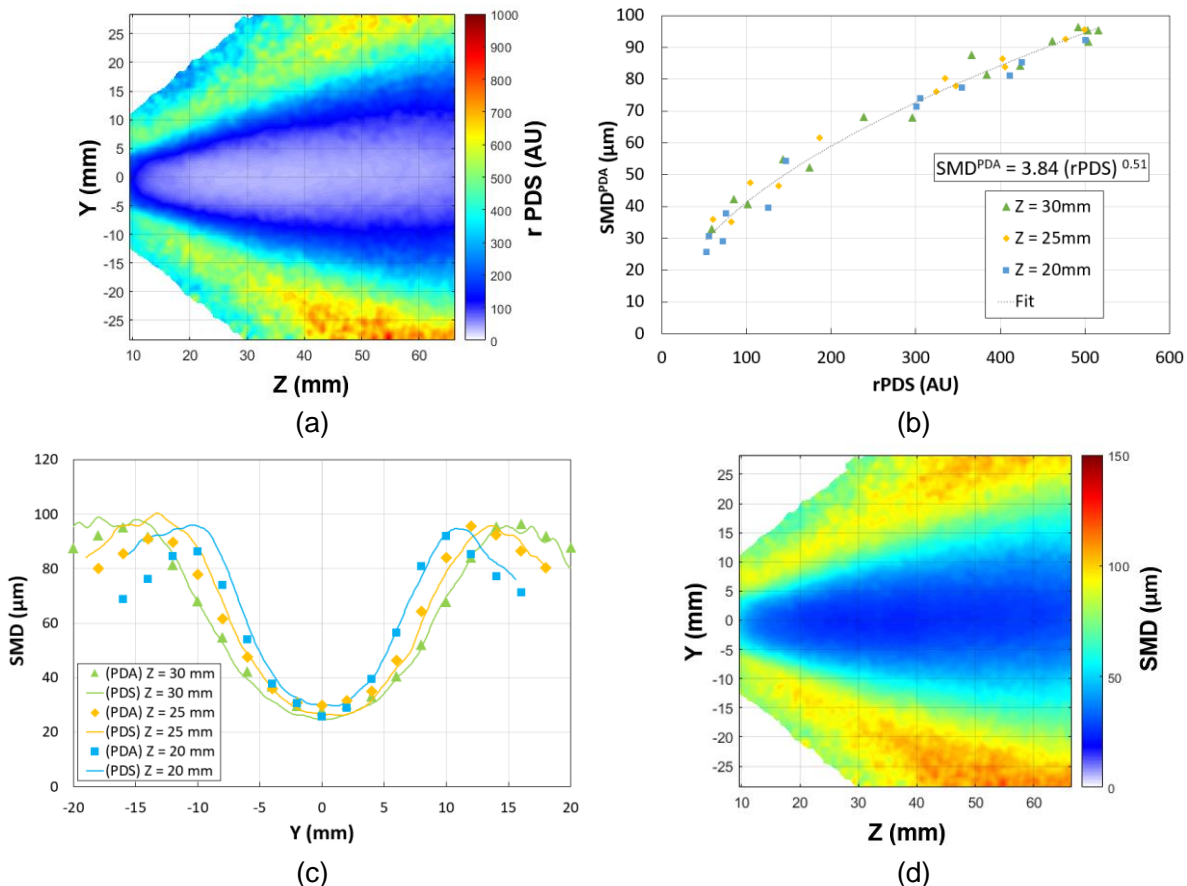


**Figure 8.** (a) LIF/Mie ratio mappings obtained with 1p-SLIPI method and average over 700 images. (b) Look-up Table linking rPDS ratios and SMD measured by PDA. (c) Comparison between SMD profiles obtained by PDA and rPDS, at several distances from the injection point. (d) Average absolute SMD map for an ethanol spray.

The application of the LUT on the PDS ratios obtained from imaging yields the SMD (PDS) profiles which can be compared to the PDA ones (**Figure 8 (c)**). As can be seen, the min/max dynamics is respected between the PDA and rPDS SMD profiles. The PDA diameter distributions are considered as a reference for this kind of experiment in two-phase flows. Vertical (Y) scans are performed with a spacing of 2 mm between points at various distances (Z) from the injector, in order to precisely locate the center of the spray in each cross-section and to check the axisymmetry. Due to the presence of irregular ligaments and non-spherical drops (due to secondary break-up and droplet coalescence further downstream), the PDA profiles were taken from Z = 15 mm to 30 mm. The mean spherical validation is greater than 90 % in the central part of the spray ( $Y = \pm 20\text{mm}$ ) and remains above 80 % elsewhere, which demonstrates the quality of the measurement. Then, the averaged 2D maps of droplet SMD is obtained by applying the LUT

on the PDS images (**Figure 8 (d)**). The average droplet SMD varies between a minimum of about 30  $\mu\text{m}$  in the center and a maximum of 100  $\mu\text{m}$  on the edges.

## Conclusion

The LIF/Mie droplet sizing technique has been improved and the results have been validated through a comparison with PDA measurements. Although the calculation of laser attenuation through the spray showed a low optical density ( $OD \ll 1$ ), the 1p-SLIPI method was implemented in the experiment in view of future tests in optically denser conditions. The analysis of the parameters influencing the Mie and LIF images confirmed that the assumptions of proportionality between particle diameter and volume/surface area were not applicable for our test conditions. It has also been demonstrated that the use of a telecentric lens is necessary. Indeed, the angular dependence of a conventional lens can generate a scattering gradient on the image field and add a significant error. Finally, a method for calibrating LIF/Mie ratio images was implemented, based on the use of a LUT, allowing to link the SMD measured by PDA and the rPDS ratio. These experimental results qualitatively illustrate the main interest of the PDS technique, which is able to reveal the influence of various spray parameters on the droplet sizing with two outstanding advantages compared to point-measurement techniques: a whole map is available with a high spatial resolution and within a reasonable time. The study thus demonstrates the strong capability of the PDS method for further industrial applications.

## Acknowledgments

The authors gratefully acknowledge the ONERA and “Région Occitanie” for funding support of the PhD.

## References

- [1] Lefebvre, A. H., McDonell, V. G., 2017, *Atomization and Sprays*, Second Edition CRC Press Taylor & Francis Group.
- [2] Yeh, C., Kosaka, H., Kamimoto, T., 1993, A fluorescence / scattering imaging technique for instantaneous 2D measurement of particle size distribution in a transient spray, *Optical Particle Sizing*, 93, pp. 4008-4013.
- [3] Felton, P. G., Bracco, F. V., Bardsley, M. E. A., 1993, On the quantitative application of exciplex fluorescence to engine sprays, *Journal of Engines*, 103, pp. 1254-1262.
- [4] Berrocal, E., Kristensson, E., Richter, M., Linne, M., Alden, M., 2008, Application of structured illumination for multiple scattering suppression in planar laser imaging of dense sprays, *Optics Express*, 16, pp. 17870-17881.
- [5] Mishra, Y., Kristensson, E., Koegl, M., Jonsson, J., Zigan, L., Berrocal, E., 2017, Comparison between two-phase and one-phase SLIPI for instantaneous imaging of transient sprays, *Experiment in Fluids*, 58 (110).
- [6] Charalampous G., Hardalupas, Y., 2011, Numerical evaluation of droplet sizing based on the ratio of fluorescent and scattered light intensities (LIF/MIE technique), *Applied Optics*, 50, pp. 1197-1209.
- [7] Findeisen, J., Gnirß, M., Damaschke, N., Schiffer, H.P. and Tropea, C., 2005, 2D Concentration Measurements Based on Mie Scattering using a Commercial PIV system, 6th International Symposium on Particle Image Velocimetry, Pasadena, California, USA.
- [8] Méès, L. and Gouesbet, G., 2001, Time-resolved scattering diagrams for a sphere illuminated by plane wave and focused short pulses, *Optics Communications*, 194, pp. 59-65.